

Triplet Test on Rubble Stone Masonry Panels



J. Milosevic, M. Lopes, R. Bento & A. S. Gago

ICIST, IST, Technical University of Lisbon, Portugal

SUMMARY

In this paper it is described an experimental research program consisting of triplet tests on nine masonry specimens with the same dimension and two types of mortar: air lime and hydraulic lime mortar. The tests were performed in three series of specimens related with three different normal pre-compression levels, according to UNI-EN 1052-3 standard, in order to obtain initial the shear strength and the coefficient of friction. Characteristic force-deformation diagrams and expected collapse mode are shown in this paper.

Aiming to reproduce the experimental tests, numerical analyses were also performed by means of nonlinear finite element models and distinct element models. The results obtained from the numerical study are compared with the experimental results and a good agreement was obtained.

Keywords: masonry buildings, triplet test, numerical analysis

1. INTRODUCTION

The structural arrangement of Lisbon old masonry buildings is based on external (peripheral) loadbearing rubble stone masonry walls, internal loadbearing masonry walls with an inner timber frame and wood pavements. The rubble stone masonry walls with lime mortars have, therefore, an important role in the structural behavior of those buildings, which is even more important when it concerns the seismic action. To assess the seismic strength of this type of buildings it is required the knowledge of the mechanical parameters that govern the shear behavior of the rubble stone masonry walls. However, experimental testing on these relevant structural elements is relatively scarce, particularly in Portugal, where experimental works for characterization of this type of constructions are rare. In the international literature it can be found some experimental results about this type of rubble stone masonry walls, which are spread throughout the Mediterranean, but the Lisbon's masonry have some local characteristics that required a particular study.

To fill this knowledge gap an extensive experimental campaign, developed within scope of the national research project SEVERES (www.severes.org), was carried out to characterize shear behavior of traditional loadbearing masonry walls. The experimental campaign on rubble stone panels included diagonal compression tests, triplet tests and cyclic tests. In the present paper are presented the results of the triplet tests performed on nine masonry specimens, which allowed calculating the masonry shear strength by means of its cohesion and friction coefficient. Even though triplet tests are usually performed on brick masonry specimens, its use on rubble stone masonry can give important information about the sliding behavior of rubble stone masonry walls.

Nine rubble masonry specimens (five with hydraulic lime mortar and four with air lime mortar) representative of the traditional Lisbon old buildings masonry walls were specially built for this experimental campaign. The specimens (40 cm height) were executed with three lime stone layers (about 13 cm height each) and two horizontal (approximately) bed joints. Those almost horizontal bed joints, to be submitted to normal and shear stresses, intend to simulate the constructive joints (at the ground floor level and at some floor levels) that can be detected in real constructions (Fig. 1.1). The tests were performed following (with adaptations) the standard recommendations for triplet tests on

brick masonry specimens (EN 1052-3 standard [BS EN, 2002] and the other works [Prota et al., 2006, Oliveira et al., 2002]).



Figure 1.1. Horizontal constructive joint at a floor level in a rubble stone masonry wall

The experimental tests were also modeled by non-linear finite element models [Diana, 2005] and distinct element models [Itasca, 2011]. The numerical results showed a good agreement with the experimental data, which allowed the calibration of the models mechanical parameters.

2. TRIPLET TESTS

2.1 Test description

To characterize the shear strength of horizontal bed joints in rubble lime stone masonry, triplet tests were performed on nine masonry specimens ($60 \times 40 \times 40$ cm). The specimens were manufactured with two types of mortar (air lime and hydraulic lime mortar) and were executed with three lime stone layers (about 13 cm height each). According to the EN 1052-3 standard [BS EN, 2002] each type of specimens was submitted to a three different pre-compression levels, which were kept constant, as much as possible, during the tests. The specimens with hydraulic lime mortar were submitted to a pre-compression level of 0.1 MPa (series 1: panels T1 and T2), a pre-compression level of 0.2 MPa (series 2: panel T5) and pre-compression level of 0.3 MPa (series 3: panels T3 and T4). Correspondingly, the specimens built with air lime mortar were subdivided into three series: series 4, for a pre-compression level of 0.1 MPa (panels T6 and T7); series 5, for a pre-compression level of 0.3 MPa (panel T8); and series 6, for a pre-compression level of 0.5 MPa (panel T9).

As is shown in Fig. 2.2, the test setup consists of two horizontal supports to restrain the horizontal movement of the top and bottom stone layers, an horizontal steel beam at the top of the specimen where acts a vertical 300 kN hydraulic jack and an horizontal 300 kN hydraulic jack acting at the middle stone layer.

The relative displacements of the specimen's stone layers were recorded with thirteen linear displacement transducers (LVDTs), which were placed on the four faces of the specimens (Fig. 2.3). Six transducers measured the horizontal relative displacements on the front and back faces (TSH4, TSH5, TSH6 on the front face and TSH7, TSH8, TSH9 on the back face) and two transducers were placed on the front and on the back faces of the specimens to measure the vertical deformation of the specimens (TSV13 on the front face and TSV12 on the back face). On the face where the horizontal load is applied it was placed one transducer at the horizontal actuator (TSH2) and two transducers to measure the horizontal displacements (TSH1 and TSH3). On the opposite face two other horizontal transducers were placed (TSH10 and TSH11).

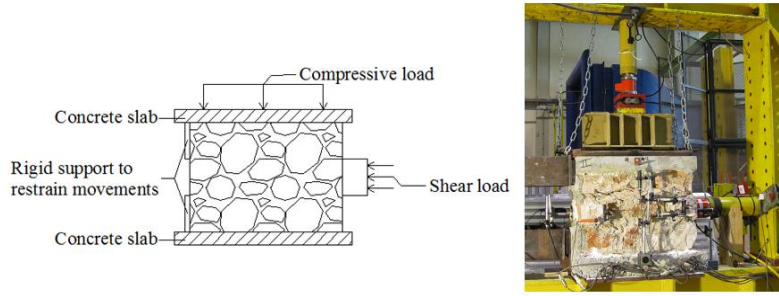


Figure 2.2. Triplet test setup – general view

The test procedure begins with the application of the vertical compressive load by the vertical hydraulic jack, which was kept constant during the complete test. It worth mention that some small unloading steps were necessary to obtain that constant vertical stress level. After reached the desire compressive load it was applied an increasing horizontal load (by the horizontal hydraulic jack), which was increased till the specimen's collapse.

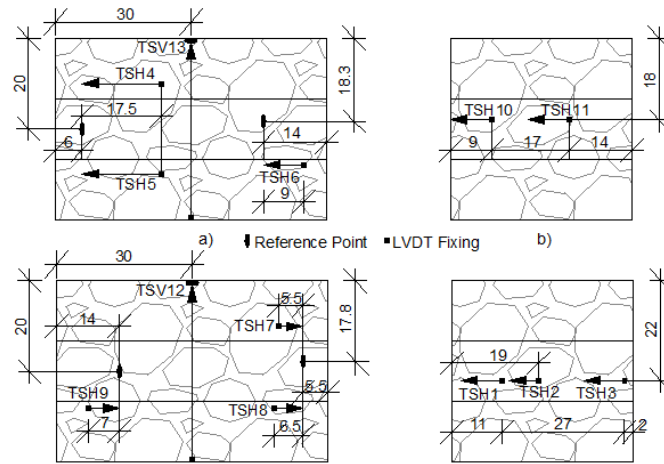


Figure 2.3. Position of transducers: (a) front and back faces; (b) Lateral faces (dimension in [cm])

The shear strength of each specimen, for the correspondent vertical stress level, can be calculated by

$$\tau_0 = \frac{F_{i,\max}}{2 \times A_i}, \text{ where } F_{i,\max} \text{ is the maximum horizontal force and } A_i \text{ is the corresponding horizontal}$$

bed joint area. On the other hand, the shear strength τ of masonry under moderate normal stresses is given by the Coulomb criterion [Vasconcelos, 2005; Hamid & Drysdale, 1980a)b); Atkinson et al., 1989; Riddington & Ghazali, 1990]:

$$\tau = \tau_0 + \mu \times \sigma \quad (2.1)$$

where μ and σ stand for coefficient of friction and vertical stress, respectively. Thus, the results obtained on the several triplet tests performed with different σ values can be used to define τ_0 and μ by means of linear regression.

2.2 Experimental Results of Triplet Tests

2.2.1 Failure modes

As already mention, nine masonry specimens were built for triplet tests. Five masonry specimens executed with hydraulic lime mortar, whereas the remaining four specimens were based on air lime

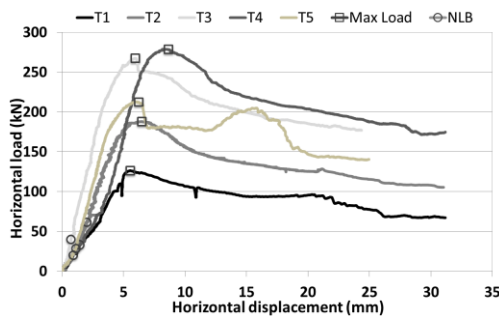
mortar. The specimens were built with three stone layers, which lead to a shear collapse mode by sliding of the medium layer. All specimens followed the expected failure pattern, which is represented in Fig. 2.4.



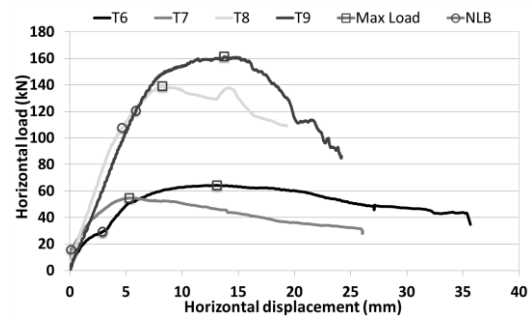
Figure 2.4. Collapse of masonry specimens: (a) specimen T1 and (b) specimen T7

2.2.2 Masonry specimens based on hydraulic lime mortar

The ‘horizontal force – horizontal displacement diagram’ (displacement measured with the transducer placed on the hydraulic actuator, TSH2) for the triplet tests on specimens built with hydraulic lime mortar (series 1, 2, 3) are depicted in Fig. 2.5(a). As can be noticed in that diagram, the ultimate loads for specimens tested with a pre-compression of 0.1 MPa were 126 kN (horizontal displacement of 5.56 mm), in specimen T1, and 188 kN (horizontal displacement 6.50 mm), in specimen T2. For a pre-compression of 0.2 MPa, the specimen T5 had an ultimate load of 213 kN (horizontal displacement of 6.09 mm). The specimens T3 and T4 were tested with a 0.3 MPa pre-compression level and the collapse loads were, respectively, 267 kN (horizontal displacement of 5.95 mm) and 279 kN (horizontal displacement of 8.42 mm). As it was expected, higher pre-compression levels produced higher shear resistances.



(a)



(b)

Figure 2.5. Horizontal load vs. Horizontal displacement: (a) Series 1, 2, 3; (b) Series 4, 5, 6
(Note: Max load – maximum load; NLB-end of linear behaviour)

It should be mentioned that in Fig.2.5 (a) and Fig.2.5 (b) are marked the points where the linear behavior ends (circle) and the points of maximum shear force (square).

2.2.3 Masonry specimens based on air lime mortar

Experimental results of the specimens built with air lime mortar (series 4, 5, 6) can be seen in Fig.2.5 (b) (shown above). In the “horizontal load – horizontal displacement diagram” (displacement measured with the transducer placed on the horizontal actuator, TSH2), are shown the ultimate shear loads for specimens tested with a pre-compression of 0.1 MPa (specimens T6 and T7), 0.3MPa (specimen T8) and 0.5 MPa (specimen T9). For specimens T6 and T7 the ultimate shear forces were, respectively, 64 kN (horizontal displacement of 13.10 mm) and 56 kN (horizontal displacement of 5.57 mm). For specimens T8 the collapse load was 139 kN (horizontal displacement of 8.23 mm). In the last specimen, T9, tested with a compression of 0.5 MPa, an ultimate load of 161 kN can be noticed (horizontal displacement of 13.75 mm). Also, as in case of hydraulic lime mortar specimens, higher pre-compression levels produced higher shear maximum loads.

In Table 2.1 are summarized the values of shear strength for all specimens.

Table 2.1. Results of Triplet Tests

Series	Panel	Type of mortar	Precompressive stress σ [MPa]	Vertical force [kN]	Maximum shear force [kN]	Shear strength τ [MPa]	Average shear strength τ [MPa]
Series 1	T1	Hydraulic	0.1	24	126	0.26	0.33
	T2				188	0.39	
Series 2	T5	Hydraulic	0.2	48	213	0.44	0.44
Series 3	T3	Hydraulic	0.3	72	267	0.56	0.57
	T4				279	0.58	
Series 4	T6	Air lime	0.1	24	64	0.134	0.13
	T7				56	0.120	
Series 5	T8	Air lime	0.3	72	139	0.29	0.29
Series 6	T9	Air lime	0.5	120	161	0.34	0.34

2.3 Discussion

In Fig. 2.6 are shown, for all tests, the relation between the normal pre-compression stress and the shear strength. In the graphic of Fig. 2.6 are also presented two straight lines, evaluated by linear regression, which pretend to represent the Coulomb shear failure criterion for each type of mortar. The good correlation between experimental results and the linear regression confirms the initial assumption of a Coulomb's friction law for shear strength. The linear regression provided the shear strength parameters of the Coulomb's friction model, namely the initial shear strength (or cohesion) τ_0 and the coefficient of friction μ . The values obtained for hydraulic lime mortar specimens were 0.20 MPa for cohesion and 1.23 for the coefficient of friction. For air lime mortar specimens the obtained values for cohesion and coefficient of friction were 0.08 MPa and 0.56, respectively.

The values obtained for cohesion are similar to the values proposed by the Italian Standard OPCM 3274 (OPCM 3274, 2003), for rubble stone lime masonry executed with air lime mortar.

According to EN 1052-3 [BS EN, 2002], the characteristic values for cohesion and coefficient of friction can be estimated as (about) 80% of the experimental values. Thus, the characteristic values for cohesion τ_{k0} are 0.16 MPa and 0.07 MPa, for hydraulic and air lime mortar specimens, respectively.

The characteristics values for the coefficient of friction μ_k are 0.98 and 0.45, for hydraulic and air lime mortar specimens, respectively. It must be mention that the obtained characteristic values for the coefficient of friction are higher that the value (0.40) proposed by the OPCM 3274 (OPCM 3274, 2003) standard and by the Eurocode 6 (EC 6, 1995) for new brick masonry. However, due to the stones imbrication in irregular lime stone masonry, a higher coefficient of friction will be expected.

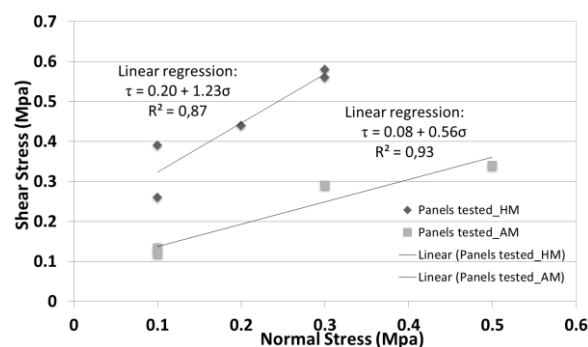


Figure 2.6. Relation between shear strength and normal stress for hydraulic and air lime mortar

3. NUMERICAL MODELING

In the present work two types of numerical models were used to simulate the triplet tests, namely a non-linear finite element model [Diana, 2005] and a distinct element model [Itasca, 2011]. Both models are able to simulate the masonry non-linear behavior, namely its shear strength and the reduced tensile strength.

In the finite element model a discrete approach was adopted. The three stone layers were modeled by nine-node continuum plane stress elements, while the mortar bed joints were simulated by six-node zero-thickness line interface elements. For the continuum elements a linear elastic behavior was adopted, being the non-linear behavior concentrated in the interface elements. The material model adopted for the interfaces was the multi-surface interface model proposed by Lourenço and Rots [Lourenço & Rots, 1997].

The distinct element method allows the explicit modeling of stones and joints, with displacement and rotations of the individual blocks. In the experimental tests modeling each stone layer was model by an individual block, with linear elastic behavior (by triangular finite differences elements). As in the previous model, the non-linear behavior was concentrated in the joints, in this case by means of non-linear contacts.

3.1 Nonlinear Finite Element Model

The multi-surface interface model proposed by Lourenço and Rots [Lourenço & Rots, 1997] is appropriate to simulate fracture, frictional slip as well as crushing along interfaces. The model assumes that the stone units behave in an elastic regime, while inelastic behavior is concentrated in the joints [Diana, 2005]. As mention, in the finite element model the stone layers were modeled using nine-node continuum plane stress elements, while the horizontal joints were represented by six-node zero-thickness line interface elements (Fig.3.7).

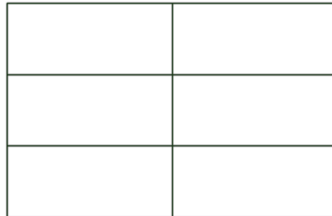


Figure 3.7. Finite element model mesh

For the finite element model it was adopted the shear strength parameters obtained by the experimental tests (i.e. coefficient of friction ($\tan \phi$) and cohesion (c)), as well as, the young modulus obtained experimentally for the vertical deformation of the stone layers. It must be mention that the for hydraulic lime and air lime mortar specimens it was found similar values for the young modulus, which means that the stones were in contact and the mortar hadn't an important influence in the deformability, at least in an early stage of vertical loading. The other interface parameters, like normal stiffness k_n , shear stiffness k_s , tensile strength f_t , fracture energies for Mode I (G_f^I) and Mode II (G_f^{II}), compressive fracture energy (G_{fc}), dilatancy coefficient $\tan \psi$, and compressive strength f_c , were defined based on other works [Senthivel & Lourenço, 2009; Oliveira, 2003; Gago et al, 2011] and by trial and error, trying to adjust the numerical results to the experimental curves. Table 3.2 and Table 3.3 summarize the elastic and inelastic parameters adopted for finite element models.

Table 3.2. Elastic properties for the continuum and interface elements

Mortar	Unit		Joint	
	E [GPa]	ν	k_n [N/mm ³]	k_s [N/mm ³]
Hydraulic	1.0	0.15	0.3	0.3
Air lime	1.0	0.15	0.07	0.07

Table 3.3. Inelastic properties for interface elements

Specimens	Tension		Shear				Compression	
	f_t [MPa]	G_f^I [$\frac{N}{mm}$]	c [MPa]	$\tan \phi$	$\tan \psi$	G_f^{II} [$\frac{N}{mm}$]	f_c [GPa]	G_{fc} [$\frac{N}{mm}$]
T3	0.1	0.1	0.2	1.23	0.001	0.5	5.0	5.0
T8	0.01	0.1	0.09	0.6	0.001	0.5	3.0	5.0

The boundary conditions and the load application were defined according to the experimental arrangement. Firstly the vertical load was applied in the upper surface and then the horizontal load was applied increasingly, till the specimen's collapse. The horizontal displacement of the right surfaces of the upper and lower stone layers were restricted, as happened in the experimental test.

As can be seen in Fig. 3.8(a) and Fig. 3.8(b) the results obtained with the finite element method shows a reasonable matching between numerical and experimental values for both the ultimate load and the initial loading branch ((Fig. 3.8(a) and Fig. 3.8(b) also show the ultimate load obtained by the distinct element method, referred later in section 3.2)). Concerning the failure mode, the numerical models agreed reasonably well with the experimental evidence, as it can be noticed in Fig. 3.9(a)(b) and Fig. 3.10(a)(b).

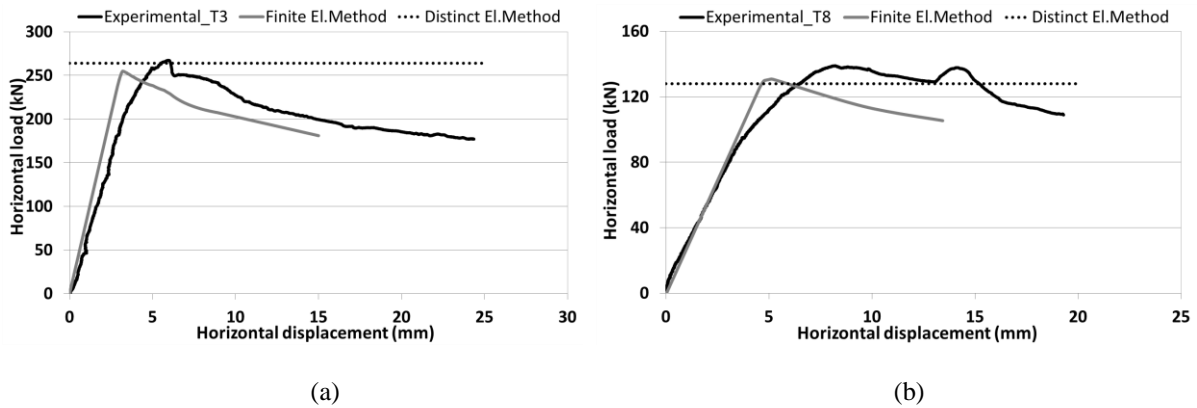


Figure 3.8. Experimental and numerical results: Force vs. Horizontal displacement: (a) Wall T3; (b) Wall T8

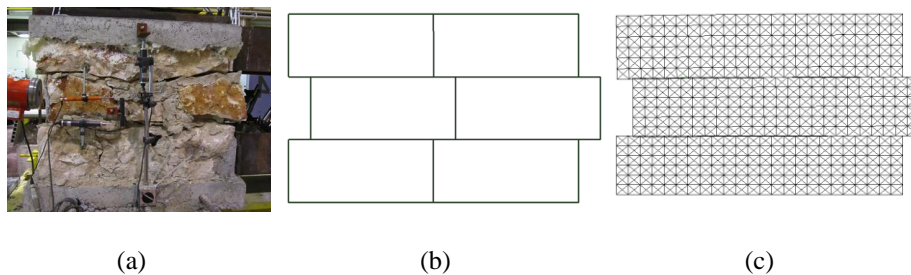


Figure 3.9. Wall T3 – Experimental and numerical failure modes: (a) Experimental; (c) Finite element model; (c) Distinct element model

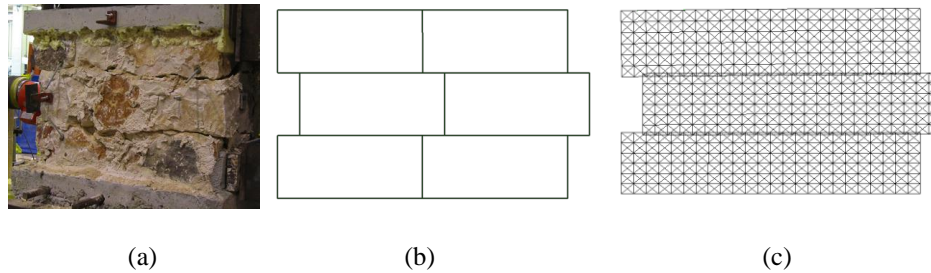


Figure 3.10. Wall T8 – Experimental and numerical failure modes: (a) Experimental; (c) Finite element model; (c) Distinct element model

3.2 Distinct Element Model

The distinct element model (Fig.3.11) consisted in a group of three blocks (each one simulating a stone layer and modeled by a finite difference elements mesh) with non-linear contacts between those block elements. For the finite difference triangular element mesh with linear elastic behavior it was adopted for the two types of specimens (hydraulic and air lime mortars) a bulk modulus (K) of 480 MPa and a shear modulus (G) of 430 MPa, which were obtained by a Young modulus (E) of 1 GPa and a Poisson's coefficient (ν) of 0.15.

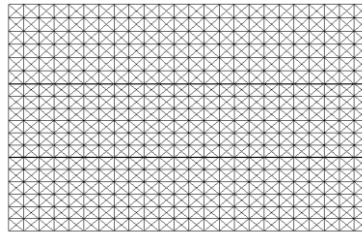


Figure 3.11. Finite element triangular mesh

An appropriate behavior was assigned for the contacts between blocks by a Coulomb slip model with residual strength. The mechanical parameters of the mentioned contact model are the normal stiffness (J_{kn}), the shear stiffness (J_{ks}), the friction angle (ϕ), the residual friction angle (ϕ_{res}) the cohesion (c), the residual cohesion (c_{res}) and the tensile strength (f_t) and the corresponding parameters for the residual strength. The joint deformability parameters (J_{kn} and J_{ks}) control the initial loading branch and the joint strength parameters (ϕ , c and f_t) control the ultimate force level. Those values were quantified considering the values obtained in the experimental tests (as in the finite element models) and by trial and error, trying to adjust the numerical and the experimental force-displacement curves. However, the trial and error procedure was based on values adopted in other works [Azevedo et al, 2000; Lemos, 2007; Gago et al., 2011]. For the residual strength after the beginning of sliding, a degradation of 40% was estimated, based on the numerical and experimental results adjustment. Table 3.4 shows the adopted values for the contacts and blocks mechanical parameters.

Table 3.4. Mechanical properties adopted for the distinct element model

Masonry specimen	Bulk modulus K [MPa]	Shear modulus G [MPa]	Normal stiffness J_{kn} [$\frac{N}{mm^3}$]	Shear stiffness J_{ks} [$\frac{N}{mm^3}$]	Friction angle ϕ [°]	Residual friction angle ϕ_{res} [°]	Cohesion c [MPa]	Residual cohesion c [MPa]	Tensile strength f_t [MPa]
T3	480	430	0.3	0.3	50	20	0.2	0.08	0.1
T8	480	430	0.07	0.07	30	12	0.09	0.036	0.01

As it can be seen in Fig. 3.8(a) and Fig. 3.8(b), for both type of wall specimens (hydraulic and air lime mortar) a good matching for the ultimate load was reached by the distinct element method. In the mentioned figures is presented only the maximum load obtained by the distinct element method, since for the software used the force-displacement curve can not be obtained, at least directly. Further developments should be done in the present work in order to obtain those curves. Finally, it worth mention that the models presented a failure pattern similar to the experimental one (Fig. 3.9(c) and Fig. 3.10(c)).

3.3 Discussion

As can be noticed, the numerical models (finite element and distinct element models), showed a good matching between numerical and experimental results for the ultimate load and collapse modes. As can be seen in Fig. 3.9 and Fig.3.10 the obtained failure patterns (sliding) in the numerical models were quite similar to ones seen on the experimental tests.

In the finite element analysis a good agreement with the experimental results was obtained for the initial branch of the “load – displacement” curve, which indicates that the elastic parameters were well estimated. Regarding the simulation of shear behavior after the maximum load, which required very small loading steps to get convergence in all steps, a good agreement was also obtained. That agreement was obtained mainly due to the values adopted for the Mode I and Mode II fracture energies, since the compressive strength and corresponding fracture energy were not relevant. The effect of dilatancy was not considered in the present finite element simulation, which requires further developments to understand its influence in the shear strength.

In the distinct element analysis the force-displacement curve cannot be directly obtained, which represents an advantage of the finite element method. However, modeling with finite element models was much more demanding in the sense that the numerical convergence required a continuous review of the convergence criteria. For the contact behavior after the sliding, a residual strength of 40% was considered. That assumption, which as a similar effect to the fractures energies considered in the finite element models, must be confirmed in further developments of the present study by the complete force-displacement curve. Also in the distinct element model the effect of the dilatancy should be study in further developments of the present study.

4. CONCLUSIONS

Masonry specimens were specially built for this experimental campaign using the traditional techniques and materials: lime stones and hydraulic lime and air lime mortars. Nine masonry specimens were tested to obtain the shear strength parameters of traditional rubble stone masonry. Differences in terms of initial shear strength, coefficient of friction and ultimate load between specimens with hydraulic and air lime mortar can be noticed: the specimens based on air lime mortar have much lower shear strength that specimens based on hydraulic lime mortar. Due to the fact that the specimens in triplet tests collapsed by sliding of mortar joints, lead to the conclusion that the mortar composition in this type of tests has a significant influence.

The linear regression defined, provided the shear strength parameters of the Coulomb's friction model, namely the cohesion and the coefficient of friction. The values of the cohesion obtained for hydraulic lime mortar specimens and air lime specimens were 0.20 MPa and 0.08 MPa, respectively, and for the coefficient of friction 1.23 and 0.56, respectively. The values reached for cohesion are similar to the values proposed by the Italian Standard OPCM 3274 (OPCM 3274, 2003), for similar masonry.

Finite and distinct elements numerical models were used to simulate the experimental tests. Both numerical models demonstrated capability to simulate the masonry behaviour in shear and lead to results similar to the experimental ones (in terms of collapse patterns and maximum loads). In the finite element model a discrete approach was adopted. The stone layers were modeled by continuum elements and the bed joints by zero-thickness interface elements. For the continuum elements a linear elastic behavior was adopted and for the interfaces the multi-surface interface model proposed by Lourenço and Rots [Lourenço, 1997] was assumed. In the distinct element model linear elastic

behavior was assumed for the blocks and for the contacts between blocks a Coulomb slip model with residual strength was assigned. With the finite elements models the complete load-displacement curves were obtained, with good agreement with the experimental results, whereas the distinct element method only yielded the maximum applied load.

Some further developments should be done on the present work, namely on the numerical models where the effect of some parameters was not completely understood. Thus, the complete force-displacement curve of the distinct element models should be obtained to evaluate the influence of the residual shear strength parameters and the effect of the dilatancy coefficient, considered zero in the present simulations, should be also studied.

ACKNOWLEDGMENTS

The authors acknowledge the financial contribution of the FCT (*Fundação para a Ciência e a Tecnologia*) project SEVERES: “Seismic Vulnerability of Old Masonry Buildings”.

REFERENCES

- Atkinson, R.H., Amadei, B.P., Saeb, S. and Sture, S. (1989). Response of masonry bed joints in direct shear. *Journal of Structural Engineering* **115:9**, 2277-2296.
- Azevedo, J., Sincraian, G., Lemos, J. V. (2000). Seismic behavior of blocky masonry structures. *Journal of Earthquake Spectra* **16:2**, 337-365.
- BS EN (2002). BS EN 1052-3, Methods of test for masonry-Part 3: Determination of initial shear strength.
- DIANA (2005). DIplacement method ANALyser, release 9.1 [CD-ROM]. *Delft, The Netherlands: TNO DIANA BV*.
- EC 6 (1995). Eurocode 6 - Design of masonry structures, part 1-1: general rules for buildings - rules for reinforced and unreinforced masonry. *ENV 1996-1-1:1995*.
- Gago, A. S., Alfaiate, J., Lamas, A. (2011). The effect of the infill in arched structures: Analytical and numerical modeling. *Journal of Engineering Structures* **33:5**, 1450-1458.
- Hamid, A. A. and Drysdale, R.G. (1980a). Behavior of brick masonry under combined shear and compression loading. *Proc. 2nd Canadian Masonry Conference*, 57-64.
- Hamid, A. A. and Drysdale, R.G. (1980b). Concrete masonry under combined shear and compression along the mortar joints. *ACI Journal* **77:5**, 314-320.
- ITASCA (2011): UDEC version 4.01 - User's guide. *Itasca Consulting Group, Inc., Minneapolis, USA*
- Lemos, J.V. (2007). Discrete element modeling of masonry structures. *International Journal of Architectural Heritage: Conservation, Analysis, and Restoration* **1:2**, 190-213.
- Lourenço, P.B. and Rots, J.G. (1997). A multi-surface interface model for the analysis of masonry structures. *Journal of Eng. Mech., ASCE* **123:7**, 660-668.
- Oliveira, J.T., Lourenço, P.B. and Barros, J.O. (2002). Shear testing of stack bonded masonry. *Report no. 02-DEC/E-10*. University of Minho, Portugal, 33.
- Oliveira, D. V. C. (2003). Experimental and numerical analysis of blocky masonry structures under cyclic loading. *Phd Thesis*, University of Minho, Portugal.
- OPCM 3274 (2003). Ordinanza del Presidente del Consiglio dei Ministri n° 3274 del 20 Marzo 2003: Allegato 2: - *Norme tecniche per il progetto, la valutazione e l'adeguamento sismico degli edifici, Italy*.
- Prota, A., Marcari, G., Fabbrocino, G., Manfredi, G. and Aldea, C. (2006). Experimental in-plane behavior of tuff masonry strengthened with cementitious matrix-grid composites. *Journal of Composites for Construction* **10**, 223.
- Riddington, J.R. and Ghazali, M.Z. (1990). Hypothesis for shear failure in masonry joints. *Proc. Instn. Civ. Engrs.* **89**, 89-102.
- Senthivel, R. and Lourenço, P.B. (2009). Finite element modeling of deformation characteristics of historical stone masonry shear walls. *Int. Journal of Engineering Structures* **31**, 1930-1943.
- Vasconcelos, G. (2005). Experimental investigations on the mechanics of stone masonry: characterization of granites and behavior of ancient masonry shear walls. *Phd Thesis*, University of Minho, Portugal.